⌘ *Author's Choice*

The Butyrylcholinesterase K Variant Confers Structurally Derived Risks for Alzheimer Pathology*⬚◆

Erez Podoly[‡§1], **Deborah E. Shalev**[§], **Shani Shenhar-Tsarfaty**[¶], **Estelle R. Bennett**[‡], **Einor Ben Assayag**[¶],
Harvey Wilgus[∥], **Oded Livnah**[‡§], and **Hermona Soreq**[‡2]

From [‡]*The Alexander Silberman Life Sciences Institute and* [§]*The Wolfson Centre for Applied Structural Biology, Safra Campus Givat Ram, Hebrew University of Jerusalem, Jerusalem 91904, Israel, the* [¶]*Department of Neurology, Sourasky Medical Center, Sackler Faculty of Medicine, Tel Aviv University, Tel-Aviv 69978, Israel, and* [∥]*PharmAthene Canada Inc., Montreal, Quebec QC H4S 2C8, Canada*

The K variant of butyrylcholinesterase (BChE-K, 20% incidence) is a long debated risk factor for Alzheimer disease (AD). The A539T substitution in BChE-K is located at the C terminus, which is essential both for BChE tetramerization and for its capacity to attenuate β-amyloid (Aβ) fibril formation. Here, we report that BChE-K is inherently unstable as compared with the "usual" BChE (BChE-U), resulting in reduced hydrolytic activity and predicting prolonged acetylcholine maintenance and protection from AD. A synthetic peptide derived from the C terminus of BChE-K (BSP-K), which displayed impaired intermolecular interactions, was less potent in suppressing Aβ oligomerization than its BSP-U counterpart. Correspondingly, highly purified recombinant human rBChE-U monomers suppressed β-amyloid fibril formation less effectively than dimers, which also protected cultured neuroblastoma cells from Aβ neurotoxicity. Dual activity structurally derived changes due to the A539T substitution can thus account for both neuroprotective characteristics caused by sustained acetylcholine levels and elevated AD risk due to inefficient interference with amyloidogenic processes.

Butyrylcholinesterase (BChE),[3] the secondary acetylcholine (ACh)-hydrolyzing enzyme, is associated with the neurofibrillary tangles and amyloid plaques characteristic of Alzheimer disease (AD) (1), which suggests that it functions as a potential AD modulator. BChE activity increases in the AD brain (2–4), where it co-localizes with β-amyloid (Aβ) fibrils (5, 6). Aβ is a 39–42-amino-acid amphiphilic peptide, derived from the transmembrane domain and extracellular region of the Aβ precursor protein (7). At high concentrations, Aβ acquires a β-sheet structure, becomes insoluble, and accumulates in neurotoxic oligomers and fibrils (8) to become the main constituent of plaques in the brain of AD patients. Recent hypotheses attribute causal roles in AD to presenilin (9), oxidative stress (10), metals (11), double hit origin (12), or mitochondrial damage (13). The alternative theories state that Aβ represents a bystander or even a protector rather than the causative factor of disease and that Aβ amyloidogenesis is secondary to other pathogenic events (14). Nevertheless, a wealth of evidence demonstrates a pivotal role for Aβ in the pathogenesis of AD, yielding the amyloid cascade hypothesis (15). According to this hypothesis, the pathological accumulation of Aβ in the brain leads to oxidative stress, neuronal destruction, and finally, the clinical syndrome of AD. It is within this context that we have studied the interactions of the Kalow variant (BChE-K) with Aβ.

The C terminus of BChE functions as a tetramerization domain (16, 17) and is responsible for its quaternary organization. Four BChE monomers are held together by the aromatic interactions of seven highly conserved aromatic residues, termed the tryptophan amphiphilic tetramerization domain (WAT) (16, 17). The WAT domain interacts with proline-rich attachment domains, either via proline-rich membrane anchor in brain neurons (18) or, in neuromuscular junctions, with cholinesterase-associated collagen Q (19). In the serum, BChE tetramerization is supported by an analogous 17-mer proline-rich peptide derived from lamellipodin (20).

Analyzing the quaternary organization of cholinesterases is a complicated task. To date, all biologically relevant crystal structures of cholinesterases have been truncated forms that lack the C terminus of the protein (21), apart from a more recent study of full-length BChE that yielded crystal packing, which did not allow C-terminal interactions among subunits and lacked electron densities in the C terminus region, indicating structural disorder Protein Data Bank (PDB) code 1VZJ (22). Of note, the crystal structure of the homologous C terminus of tetrameric synaptic acetylcholinesterase (AChE-S) could only be determined based on synthetic peptides derived from the sequence of the AChE-S tail and stabilized with a proline-rich attachment domain (23).

In addition to the "usual" (BChE-U) form, BChE has nearly 40 genomic variants. The most common is BChE-K, with allelic frequencies of 0.13–0.21. BChE-K includes a single nucleotide

---

[3] The abbreviations used are: BChE, butyrylcholinesterase; BChE-K, Kalow variant of BChE; BChE-U, usual BChE; rBChE-U, recombinant rBChE-U; BSP, BChE-derived synthetic peptide; ACh, acetylcholine; AChE, acetylcholinesterase; AChE-S, synaptic AChE; ATCh, acetylthiocholine; AD, Alzheimer disease; Aβ, β-amyloid; polyP, poly-L-proline; bis-ANS, 4,4′-dianilino-1,1′-binaphthyl-5,5′-sulfonate; TTR, Transthyretin; LDH, lactate dehydrogenase; TEM, transmission electron microscopy; ThT, thioflavin T; Tricine, N-[2-hydroxy-1,1-bis(hydroxymethyl)ethyl]glycine; DMSO, dimethyl sulfonate.

polymorphism at position 1699 (single nucleotide polymorphism data base (dbSNP) ID: rs1803274; alleles, A/G). This leads to an alanine-to-threonine substitution at position 539, 36 residues upstream to the C terminus of BChE (24), within the tetramerization domain that we previously found to attenuate amyloid fibril formation (25).

Ample evidence supports the importance of alanine-to-threonine substitutions and their relevance to amyloidogenic processes, protein stability, and quaternary organization (supplemental Table ST1). Point mutations at the dimer interface of light chain immunoglobulins decrease their stability so that the A34T polymorphism in this protein leads to systemic amyloidosis (26). An A25T mutant of the tetrameric human protein Transthyretin (TTR), associated with central nervous system amyloidosis, is prone to aggregation and exhibits drastically reduced tertiary and quaternary structural stabilities (27). The thermodynamic stability profile of the A25T TTR mutant shows that both monomers and tetramers of this variant are highly destabilized. In addition, A25T TTR tetramers dissociate very rapidly (about 1200-fold faster than the dissociation of wild-type TTR), reflecting a high degree of kinetic destabilization of their quaternary structure. These factors together probably contribute to the high propensity of A25T TTR to aggregate *in vitro*.

The capacity of serum BChE-K to hydrolyze butyrylthiocholine was reported to be reduced by 30% relative to BChE-U, for yet unclear reasons (24). The reduced hydrolytic activity of BChE-K predicts that BChE-K carriers would potentially sustain improved cholinergic transmission as compared with BChE-U carriers and has been shown to correlate with preserved performance of attention and reduced rates of cognitive decline (28). However, BChE-K carriers are refractory to cholinesterase inhibitor therapy, the current leading treatment of AD (29). This raised the question whether BChE-K functions as an AD risk or protection factor. Genotype studies are controversial, with some showing increased risk of AD for homozygote BChE-K carriers (*e.g.* Ref. 30), whereas others suggest a protective effect (*e.g.* Ref. 31). A recent meta-analysis concluded that on average, BChE-K is neither a risk factor nor a protection factor for AD (32). Based on our previous findings of the arrest of Aβ fibril formation by BChE and considering the accumulation of monomeric BChE in the most severe AD cases (33), we used a variety of chemical techniques to study the effect of the A539T substitution on BChE stability and tetramerization on the one hand and on its potency in attenuating Aβ oligomerization and fibril formation on the other.

EXPERIMENTAL PROCEDURES

Subjects—321 (184 males, 137 female) healthy individuals (mean $\pm$ S.D. age: 65.99 $\pm$ 11.11 years) from various out-patient clinics of the Tel-Aviv Sourasky Medical Center were enrolled during the period from February 2001 to September 2004, as described (34). Written informed consent, approved by the local ethics committee (consent form 00-116), was obtained from all participants.

Gene Polymorphism Analysis—Genomic DNA was extracted from nucleated blood cells. For single nucleotide polymorphism analysis, a 214-bp PCR product was amplified using the forward primer 5′-CTGTACTGTGTAGTTAGAGAAAAT-GGC-3′ (nucleotide −105 to −79 upstream to the intron 3/exon 4 boundary) and the reverse primer 5′-CTTTCTT-TCTTGCTAGTGTAATCG-3′ (nucleotides 1709-1686). A fluorescein-labeled anchor probe (5′-CCAGCGATG-GAATCCTGCTTTCC-3′-FLU (fluorescein), nucleotides 1628–50) and a one base apart LC-Red-640-labeled detection probe (5′-CTCCCATTCTGCTTCATCAATATT-3′-PHO (phosphate), nucleotides 1603-26) were used as reported previously (35).

Serum Cholinesterase Analysis—Acetylthiocholine (ATCh) hydrolytic activities were assessed in a microtiter plate assay as described, with or without the selective BChE inhibitor iso-OMPA (tetra(monoisopropyl)pyrophosphorotetramide) (36). Calculated BChE ATCh hydrolytic activity was defined as the total serum ability to hydrolyze ATCh after subtraction of AChE hydrolytic activity. For stability tests, serum-derived samples of genotyped KK, UK, and UU carriers, diluted 1:10 in saline, were incubated overnight in 0–2 M urea at 37 °C and electrophoretically separated (2 h, 4 °C) in 6% non-denaturing polyacrylamide gels. This was followed by activity staining with 3.0 mM copper sulfate, 0.5 mM potassium ferricyanide, 10 mM sodium citrate, 1.6 mM *S*-butyrylthiocholine iodide, and 65 mM phosphate buffer, pH 6.0, at room temperature (37).

Statistical Analysis—Continuous data were summarized and displayed as mean $\pm$ S.D. Distributions of calculated BChE activities were assessed by the Kolmogorov-Smirnov Normality test. The difference between genotypes of mean calculated activities was evaluated using Student's *t* test; $p < 0.05$ was considered statistically significant. SPSS for Windows (version 15.0, SPSS Inc.) software was used to carry out all statistical analyses.

Peptides—Peptides used were: Aβ_{1-40}, (Sigma, Jerusalem, Israel), BSP-U and BSP-K, derived from the C-terminal sequences of human BChE (EC 3.1.1.8.) variants (U, GNIDE-AEWEWKAGFHRWNNYMMDWKNQFNDYT; K, A6T), and the 17-mer poly-L-proline (PolyP) sequence (PPPPPPPPP-PPPPPPLP), derived from lamellipodin, which promotes the assembly of BChE into tetramers (20) (GenScript Corp., Piscataway, NJ). All peptides were purified to >90%, as validated by mass spectrometry analyses.

Surface Plasmon Resonance—The ProteOn™ XPR36 protein interaction array system (Bio-Rad, Haifa, Israel) was used to study the interaction of a recombinant full-length BChE (rBChE-U) and the peptides BSP-U and BSP-K, with a polyclonal antibody raised against rBChE-U (38). The protein and peptides were immobilized on GLC chips (Bio-Rad) using standard amine coupling. Arbitrary units (resonance unit) values of binding to the chip were 6000, 900, and 600, respectively. The antibody, as analyte, was diluted serially in phosphate-buffered saline containing 0.005% Tween 20 and injected at five concentrations (3.12–50 μg/ml). All interactions were carried out at 25 °C. Immobilized IgG was used as a reference for background subtraction.

NMR-derived Solution Analysis of BSP Peptides—Peptides were dissolved in 60% d_6-DMSO (Aldrich) in double distilled water with 0.03 weight percent NaN$_3$ and measured at 29 °C. BSP samples were measured alone and with PolyP at a 4:1 molar
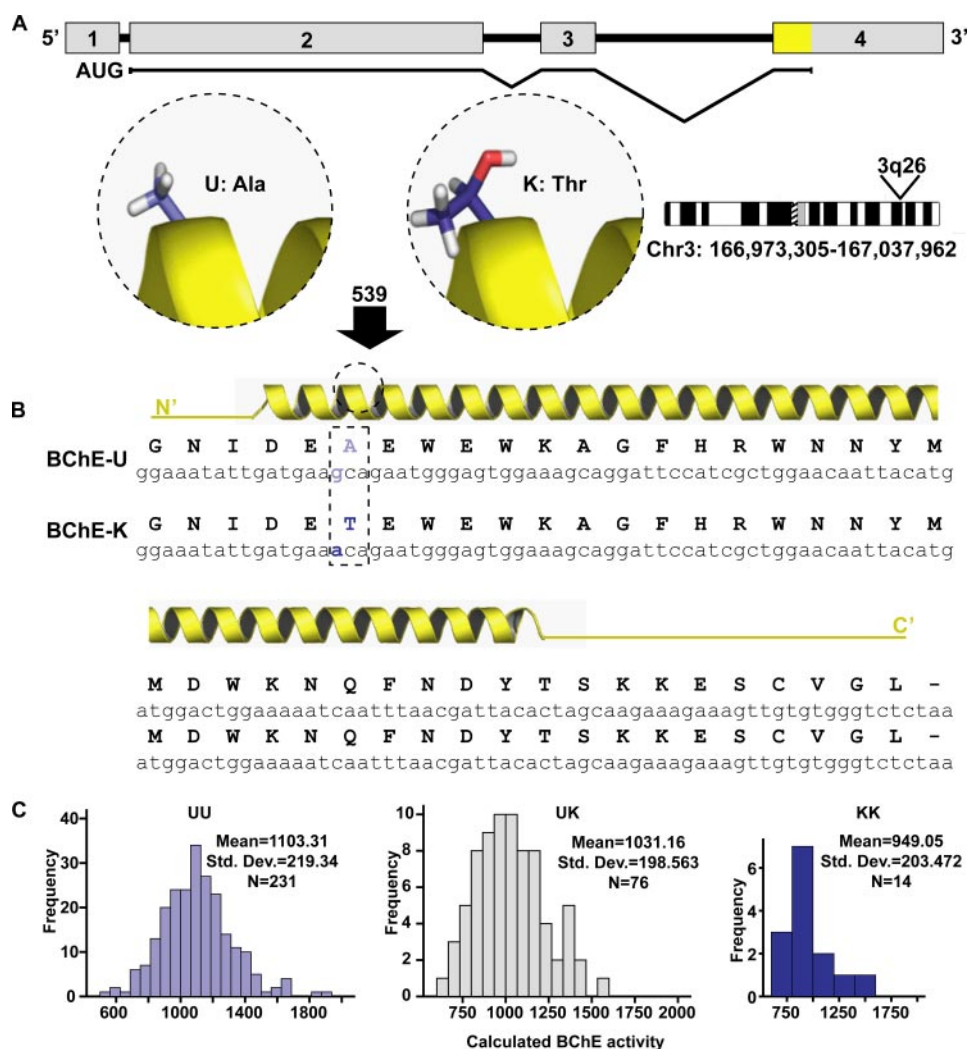
FIGURE 1. **The *BChE* gene and its usual U and K variant protein products.** *A*, BChE location on chromosome 3q26.1-q26.2 and its gene structure (56). *B*, the C-terminal DNA and amino acid sequences of BChE-U and -K. The predicted secondary structure of the amino acid substitution (enlarged) is shown above the sequences. *C*, histograms of measured BChE activity in apparently healthy carriers of the UU, UK, and KK genotypes. Units are nmol of acetylthiocholine hydrolyzed/min/ml serum.

with a shifted squared sine bell window function in both dimensions were applied prior to Fourier transformation. The baseline was further corrected in the F2 dimension with a quadratic polynomial function. Resonance assignment followed the sequential assignment methodology developed by Wüthrich (41).

Aβ Oligomerization—Oxidative photo-induced cross-linking of unmodified proteins (42) was used to study the effect of BSP peptides on Aβ oligomerization. Aβ was preincubated in hexafluoroisopropanol (Acros Organics, Geel, Belgium), lyophilized and redissolved in double distilled water to a final concentration of 100 μM. Aβ was incubated alone or in the presence of 1 μM protein or peptides over 24 h at room temperature. Aliquots were removed at 0, 4, 7, 8, and 22 h and centrifuged (30 min, 14,000 rpm). Soluble fractions were treated as described previously (43). Thioflavine T and bis-ANS fluorescence measurements and transmission electron microscopy were done as described (25, 43).

Circular Dichroism Measurements—Direct CD spectra were recorded using a CD Jasco J-810 spectropolarimeter (Easton, MD) in 1-mm path length quartz cuvettes, Hellma 100-QS (Hellma GmbH & Co. KG, Mülheim/Baden, Germany). Recordings were at 0.1-nm intervals in a spectral range of 185–260

nm. The CD spectra were computationally deconvoluted, using the K2D analysis program (44). The concentration of BSP peptides was below the level of detection so that the spectra measured changes in Aβ only.

Cell Culture—Human neuroblastoma SH-SY5Y cells (ATCC, Manassas, VA) were grown in a 1:1 mixture of minimal essential medium (Sigma-Aldrich, Rehovot, Israel) and Ham's modified medium F-12 (Sigma), with 10% fetal bovine serum (Biological Industries, Beit-Haemek, Israel). Cells were plated in 24-well plates (Nunc, Roskilde, Denmark) at 10^5 cells/well in 500 μl of medium and allowed to attach overnight. Aβ was preincubated for 4 h, diluted 1:10 (final volume 500 μl) with phenol red-free RPMI 1640 (Sigma) containing 10% serum, and added to the cells. Cell viability was determined using lactate dehydrogenase (LDH) release assays (45) as described (38).

RESULTS

BChE-K Shows Reduced Stability and Hydrolytic Activity—The BChE genotype (Fig. 1, *A* and *B*) was determined using

ratio (verified by relative peak-ratios in NMR spectra). The pH was titrated to 5.10 ± 0.05 for all samples. NMR experiments were performed on a Bruker Avance 600 MHz DMX spectrometer operating at the proton frequency of 600.13 MHz, using a 5-mm selective probe equipped with a self-shielded xyz-gradient coil. The transmitter frequency was set on the hydrogen-deuterium exchange in water signal, which was calibrated at 4.735 ppm. total correlation spectroscopy, using the MLEV-17 pulse scheme for the spin lock (39), and nuclear Overhauser effect spectroscopy (40) experiments were acquired under identical conditions for all samples, using gradients for water saturation. The nuclear Overhauser effect spectroscopy experiments were acquired with a mixing time of 200 ms.

Spectra were processed and analyzed with the XWINNMR (Bruker Analytische Messtechnik GmbH) and SPARKY3 software.[4] Zero filling in the F1 dimension and data apodization

---

[4] T. D. Goddard and D. G. Kueller, University of California, San Francisco, CA, personal communication.
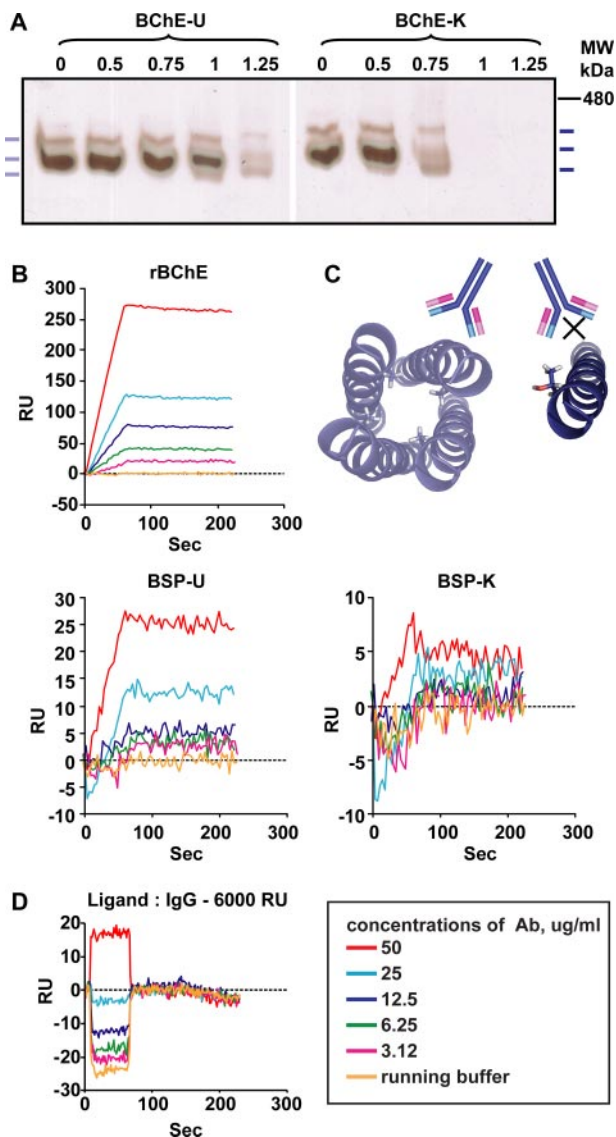
FIGURE 2. **BChE and derived peptides differ in stability and antibody recognition.** *A*, native gel subjected to activity staining of homozygous BChE-U and -K serum samples following incubation in the noted molar concentrations of urea. *B*, surface plasmon resonance analyses. Polyclonal anti-rBChE-U antibodies in the noted concentrations were injected against immobilized rBChE-U, BSP-U, and BSP-K. Signals are dose-dependent. Note the 10-fold resonance unit scale difference between rBChE-U and BSP-U signals and the lack of detectable interaction with BSP-K. *C* and *D*, positive surface plasmon resonance response of BSP-U but neither BSP-K nor IgG. Note the exceedingly low response scale despite adding 6000 resonance units (*RU*) of IgG, attesting to the specificity of the observed response with the anti-BChE antibodies (*Ab*).

FIGURE 3. **PolyP-induced NMR chemical shift deviations.** NMR-measured chemical shift differences between spectra of BSP-U and -K bound and nonbound to PolyP (shown as a *central thread* in the structure) are displayed. *Right*, location of residues that showed significant chemical shifts on the BSP structure (built according to PDB structure 1VZJ) are colored in *pink*. Residues near the kink of the helix at Gly-546 (in *blue*) were significantly shifted in both BSP peptides.

nucleated blood cell DNA from apparently healthy volunteers who also donated serum for hydrolytic activity measurements. The observed genotype distribution included 72.0% UU, 23.2% UK, and 4.4% KK variants, consistent with the Hardy-Weinberg equilibrium. The corresponding mean calculated ATCh hydrolytic activities of serum BChE from these subjects were 1103.31 ± 219.34, 1031.16 ± 198.56, and 949.05 ± 203.47 ($p = 0.011$) (Fig. 1*C*). The decline in ATCh hydrolytic activity from heterozygous to homozygous carriers indicated gene dose dependence.

The location of the A539T substitution in the C terminus, which is distant from the hydrolytic site of the enzyme, sug-
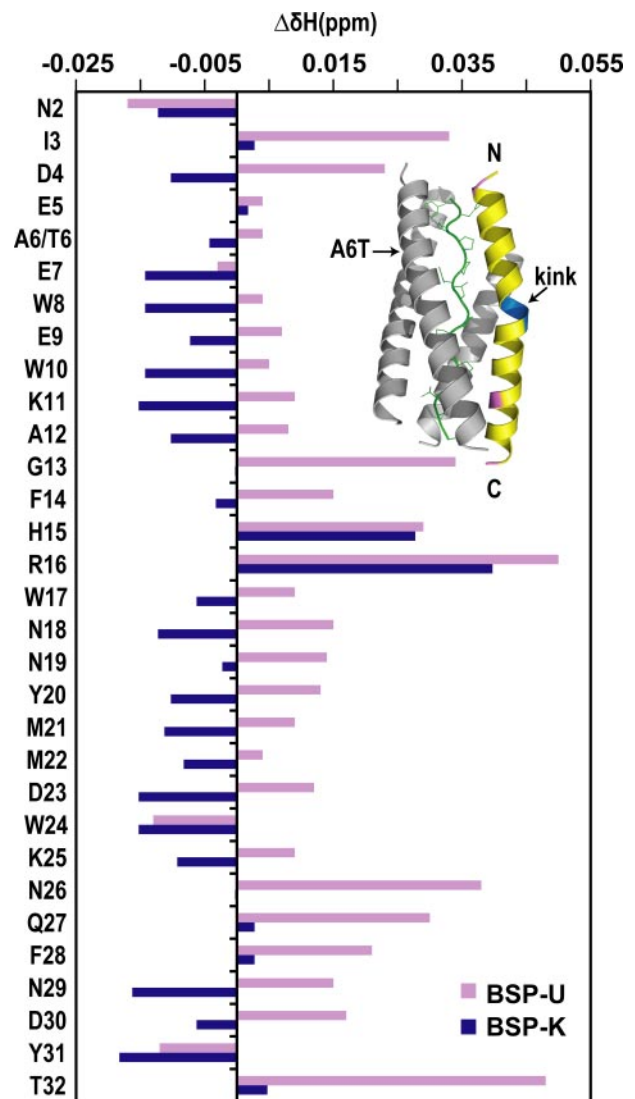
gested that its impaired stability caused the reduced activity. To challenge this prediction, the inherent stability of BChE-U and BChE-K was compared by incubating serum samples from genotyped subjects in increasing concentrations of urea followed by native gel electrophoresis and activity staining (Fig. 2*A*). Both BChE-U and BChE-K are enzymatically active tetramers; however, the enzymatic activity of BChE-K tetramers was greatly reduced following incubation in 1 M urea, unlike BChE-U, which was resistant to this treatment. This suggested that the hydrolytic activity was rapidly lost once BChE-K tetramers disassemble.

BSP Peptides Show NMR Spectral Differences—We investigated the structural origin for the instability of BChE-K by analyzing the corresponding 32-residue synthetic peptides, BSP-K and BSP-U, for their interaction with a polyclonal rabbit antibody elicited toward intact rBChE-U (46). Surface plasmon res-
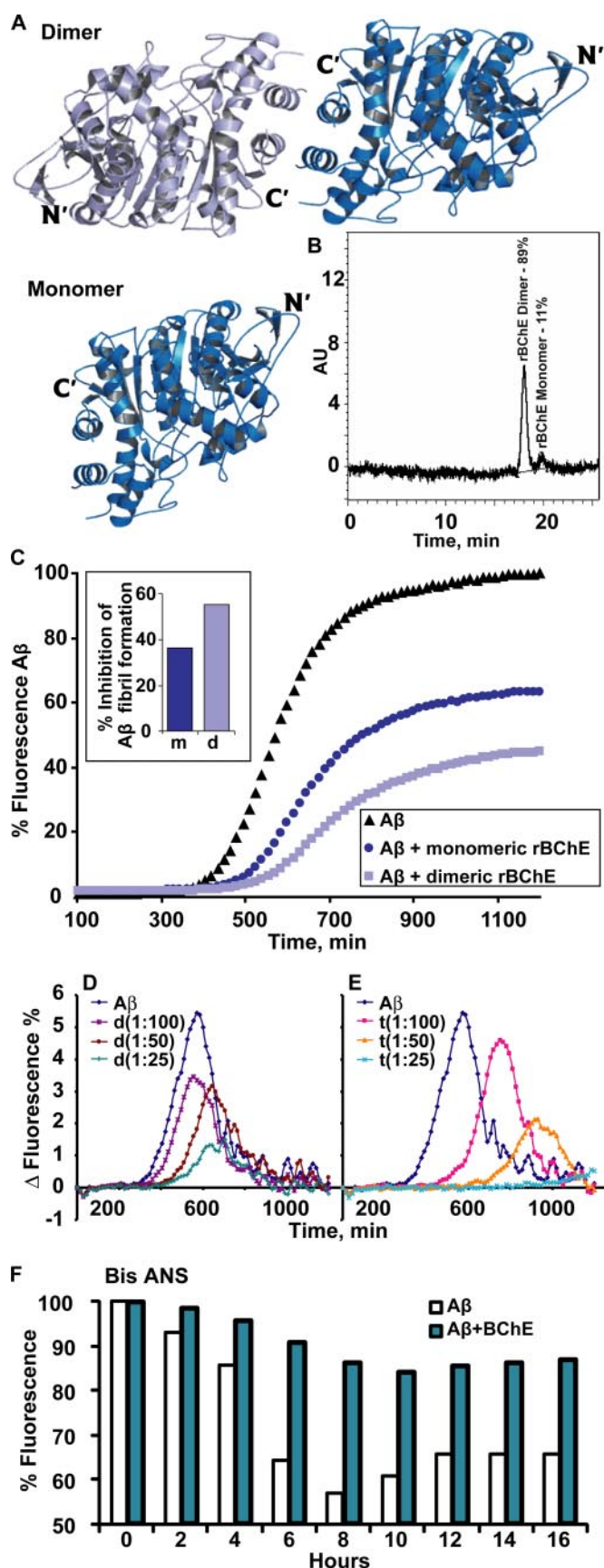
FIGURE 4. **rBChE-U dimers attenuate Aβ fibril formation more effectively than monomers.** *A*, initial dimer and monomer content in rBChE-U preparation. *B*, modeled BChE-U monomers and dimers built according to PDB struc-

onance analysis demonstrated a dose-dependent interaction of anti-rBChE-U antibodies with rBChE-U and BSP-U (albeit less profoundly) but not with BSP-K (Fig. 2, *B* and *C*). Immunoglobulin G, which does not bind to the antibody against rBChE-U (Fig. 2*D*) served as an immobilized control employed as a subtractable "baseline" in all cases. Additionally, other injected proteins (*e.g.* RACK1) did not bind rBChE or the two peptides (data not shown). These results supported the concept of structural differences between these two peptides and suggested that distinct tetramerization capacities are involved. Interactions of BSP peptides were studied by incubating them with the synthetic PolyP peptide, which facilitates BChE tetramerization (20). NMR was used to follow both BSP peptides interactions with PolyP by tracking chemical shift deviations in the amide-aliphatic interactions (fingerprint region). Because PolyP fortunately has no amide protons (apart from one leucine), it does not appear in the fingerprint region of the BSP spectra.

The spectrum of BSP-U was assigned based on total correlation spectroscopy and nuclear Overhauser effect spectroscopy spectra acquired under identical conditions and was the basis for assignments of both BSP peptides with 4:1 ratios of peptide to PolyP (see supplemental Figs. SF1– 4: supplemental Fig. 1, BSP-U; supplemental Fig. 2, BSP-U+PolyP; supplemental Fig. 3, BSP-K; supplemental Fig. 4, BSP-K+PolyP). Deviations of amide chemical shifts of each peptide in interaction with PolyP *versus* the free state are summarized in Fig. 3.

Upon adding PolyP, BSP-U showed mainly upfield chemical shift deviations, suggesting that the amide protons are more shielded in this variant when interacting with PolyP. The amide protons of BSP-K showed the opposite, except for residues His-15 and Arg-16, which were shielded, and Asn-2, Trp-24, and Tyr-31, which were deshielded in both peptides. The distinct interactions observed for these peptides with PolyP suggested inherent differences between their tetramerization potency, compatible with the reduced stability of BChE-K as compared with BChE-U.

rBChE-U Monomers Suppress Fibril Formation Less Effectively than Recombinant Dimers or Native BChE Tetramers— The C-terminal domains of both BChE dimers and monomers are relatively exposed to the surrounding environment, as modeled based on the tetrameric structure of AChE-S (Fig. 4*A*). Separate fractions of BChE dimers and monomers were used to compare the effects caused by these C termini. rBChE-U production in the milk of transgenic goats yielded primarily dimeric protein, with ~10% monomeric fraction, as shown by mass spectrometry (46) (Fig. 4*B*). Column chromatography was used to separate monomers from dimers. ThT fluorescence measurements showed that isolated fractions of highly purified rBChE-U monomers and dimers both attenuated fibril forma-

ture 1EEAY of the tetrameric structure of AChE-S. *AU*, arbitrary units. *C*, ThT fluorescence demonstrating that highly purified dimers of rBChE-U suppressed Aβ fibril formation more efficiently than monomeric rBChE-U. *Inset*, percentage of attenuated Aβ fibril formation elicited by monomers (*m*) and dimers (*d*). *D* and *E*, rates of fluorescence changes demonstrating the difference in the capacity for attenuating fibril formation by human recombinant rBChE dimers (*d*) or serum-derived tetramers (*t*). *F*, bis-ANS kinetics demonstrating an apparently similar time scale and sustained fluorescence signal in the presence of bis-ANS as compared with the suppressed signal with ThT, both supporting our working hypothesis.
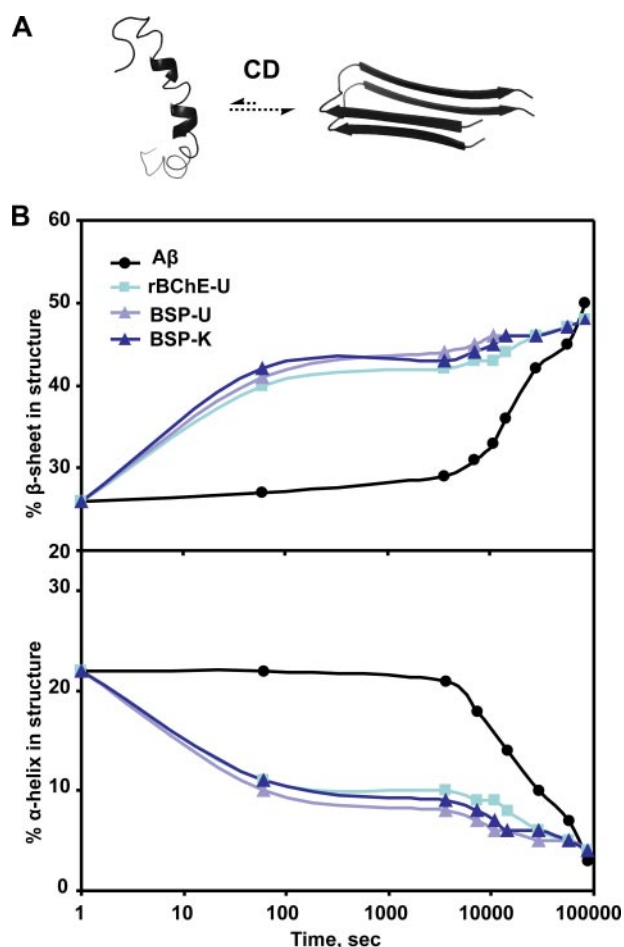
FIGURE 5. **CD evidence for BChE-accelerated conversion to β-sheet conformation.** CD deconvoluted spectra demonstrate a rapid increase in β-sheet content (*upper plot*) and rapid decrease in helical content (*lower plot*) with the addition of rBChE-U, BSP-U, and BSP-K, as compared with the increase in β-sheet content seen with Aβ alone.

FIGURE 6. **BSP-K sustains less cross-linked Aβ oligomers in solution than BSP-U.** *A*, 16% Tris-Tricine gel demonstrating BSP peptide interference with oligomerization of Aβ. *MW*, molecular weight markers; *no CL*, no cross-linking. *B*, the cross-linking reaction. *Prot*, protein. *C*, quantification of Aβ dimers and trimers in solution, in the presence of BSP-K and BSP-U.

tion at a molar ratio of 1:100 to Aβ. However, monomeric and dimeric rBChE-U showed different durations of the lag and growth phases in the fibril formation process (Fig. 4*C*). Dimeric rBChE-U attenuated Aβ fibril formation more than the monomeric BChE and presented a longer lag time and 20% less fluorescent signal at the plateau (Fig. 4*C* and *inset*). Furthermore, calculating the rate of fibril formation revealed that recombinant BChE dimers (Fig. 4*D*), and yet more so, native BChE from human serum (Fig. 4*E*) attenuate this process, suggesting direct association of this rate with the number of enzyme subunits. Inversely, a bis-ANS response curve to rBChE interaction with Aβ showed an apparently similar time scale and sustained fluorescence signal, unlike the reduced signal in the thioflavin T tests (Fig. 4*F*), both supporting our working hypothesis.

The distinct structural features of BSP-K could potentially impair its ability to modulate Aβ conversion to β-sheet conformation. This was assessed by incubating Aβ alone or with BSP peptides and following the CD spectrum for 24 h. Deconvoluted spectra of Aβ samples incubated alone showed a gradual increase in the content of β-sheets, from 26 to 50% within 2.5 h. In contrast, adding rBChE-U or BSP peptides to Aβ accelerated the increase in β-sheet content, which reached an apparent plateau within seconds (50 s, to 48%) (Fig. 5).
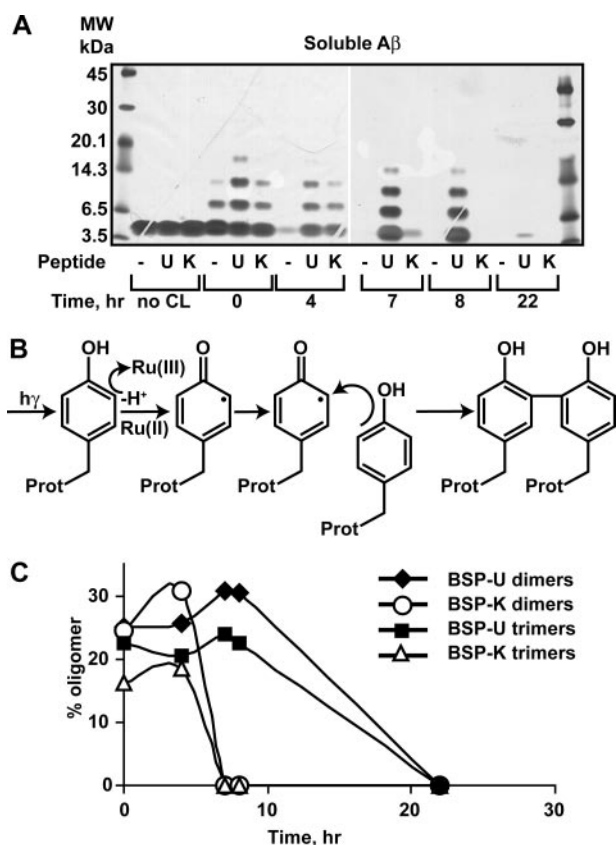
BSP-K Attenuates Aβ Oligomerization Less Effectively than BSP-U—Further studies of Aβ oligomerization involved cross-linking of Aβ in the presence or absence of BSP-U or BSP-K and separation of the soluble fractions by SDS-PAGE (Fig. 6). Aβ alone precipitated rapidly, within 4 h. Both BSP peptides prolonged the time Aβ oligomers remained in solution, but BSP-U prolonged the persistence of amyloid oligomers in solution more effectively than BSP-K; after 8 h of incubation, no oligomeric forms of Aβ remained in the soluble phase in the presence of BSP-K, whereas in the presence of BSP-U, they lasted nearly 22 h. This supports the view that BSP-K is less capable of interacting both with PolyP and with Aβ than BSP-U.

rBChE-U Attenuates Aβ Fibril Formation and Induces Fibril Disassembly—Transmission electron microscopy (TEM) was used to quantify longer and more developed Aβ fibrils, formed in the presence or absence of rBChE-U and BSP peptides. Following 48 h of incubation, Aβ alone formed mostly 50–60-nm-long fibrils, with some fibrils reaching up to 300 nm. In the presence of either of the BSP peptides, however, the majority of Aβ fibrils were 20–30-nm long with none longer than 120 nm. In the presence of rBChE-U, a dramatic reduction in the formation of fibrils of all length groups was seen, as compared with Aβ incubated alone or with BSP peptides (Fig. 7*A*).

Kinetics of TEM showed a pronounced decrease over time both in the number and in the degree of branching of the fibrils in the presence of the peptides relative to incubation of Aβ
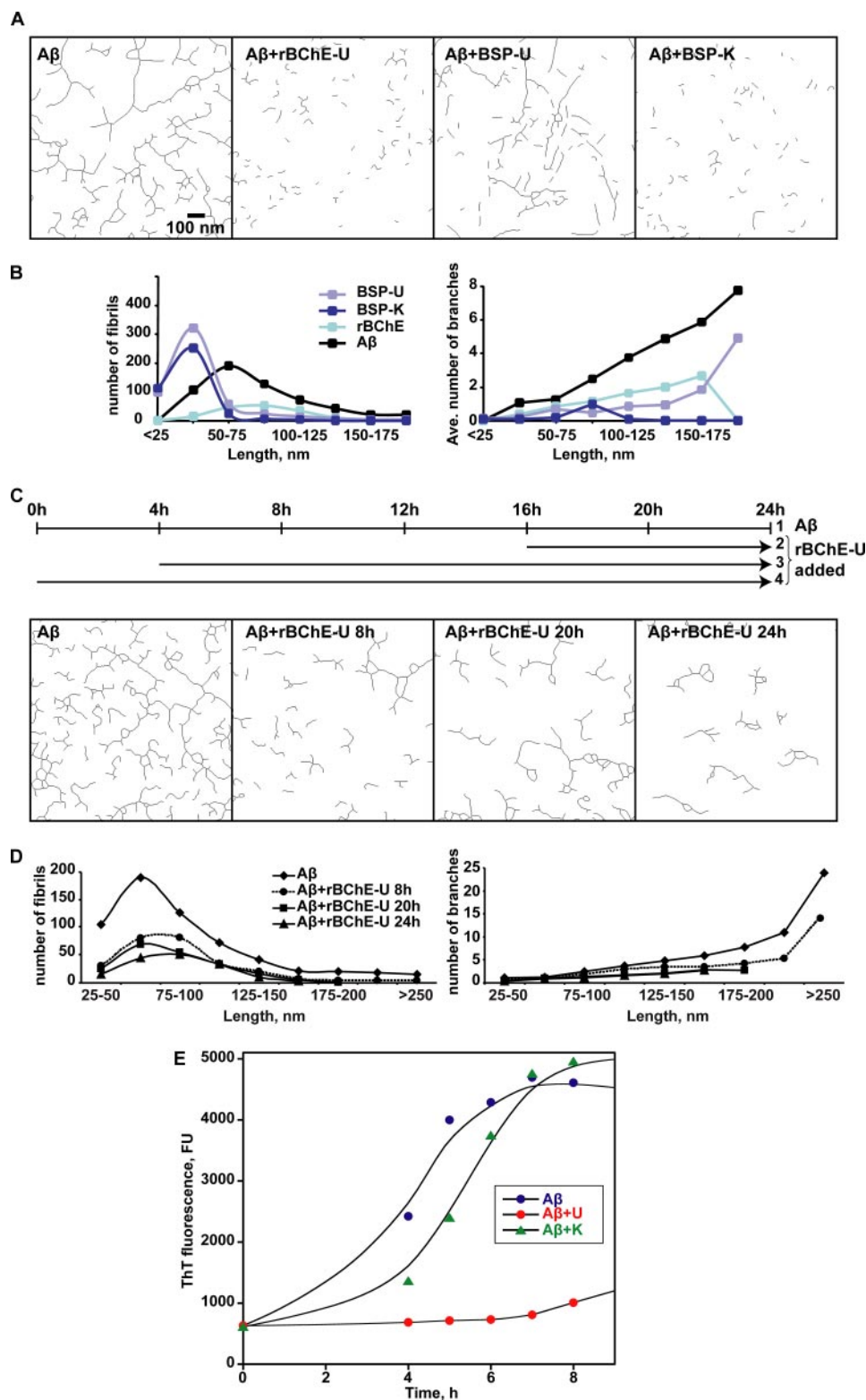
FIGURE 7. **rBChE-U attenuates fibril formation more than BSP peptides and induces fibril disassembly.** *A*, computer-processed TEM photomicrographs following 24-h incubations of Aβ alone or with BSP-U, BSP-K, or rBChE-U. *B*, fibrils were clustered into groups according to their length. Note that both BSP peptides shifted the Aβ fibrils from relatively long to numerous short fibrils, whereas rBChE-U suppressed the formation of fibrils of all length groups. *C* and *D*, Aβ alone or with rBChE-U added after different incubation times (shown by *arrows*). Plots present the fibril number or branches *versus* fibril length. Note the apparent disassembly of preformed fibrils. *E*, ThT fluorescence curves for the BSP-U and the BSP-K peptides. Note that BSP-U, but not BSP-K, was capable of repressing the ThT increment induced by Aβ. *FU*, fluorescence units.

alone. Adding rBChE-U at any time after initiation substantially further reduced the number of fibrils in a manner dependent on the duration of rBChE-U incubation for all fibril length fractions. Also, adding rBChE-U decreased the extent of branching. Fig. 7, *A–D*, present these analyses and the corresponding quantifications, demonstrating active disassembly of fibrils by rBChE-U. Of note, ThT fluorescence measurements showed suppressed increment in the presence of BSP-U, but not BSP-K (Fig. 7*E*), demonstrating a principal difference between these two peptides.

BSP Peptides Are Poor Neuroprotectors as Compared with rBChE-U— Cytotoxicity of Aβ has been attributed to low molecular weight oligomers (47, 48). Therefore, Aβ cytotoxicity and the cytoprotection provided by BSP peptides and rBChE-U was tested on cultured human neuroblastoma SH-SY5Y cells. The cells were incubated alone, in the presence of Aβ and in the presence of Aβ with BSP peptides or rBChE-U. After 72 h, an LDH release assay for cell viability showed a 26% increase in LDH release from Aβ-treated cells as compared with controls. rBChE-U prevented 85 ± 8% of this Aβ-induced LDH increase, indicating that it protects the cells from the Aβ-dependent toxicity. The BSP peptides yielded only small, variable (10–17%) changes in LDH release, suggesting that they can only function to attenuate Aβ fibril formation as an integral part of the intact BChE protein.

DISCUSSION

Various chemical and biological approaches were combined to explore the role of the BChE-K variant in Aβ accumulation, which characterizes AD pathophysiology. Our findings attribute many of the features observed for BChE-K carriers in AD to structural origins. We found BChE-K to be inherently unstable as compared with BChE-U, which may induce elevated ACh levels in its carriers, thereby delay-
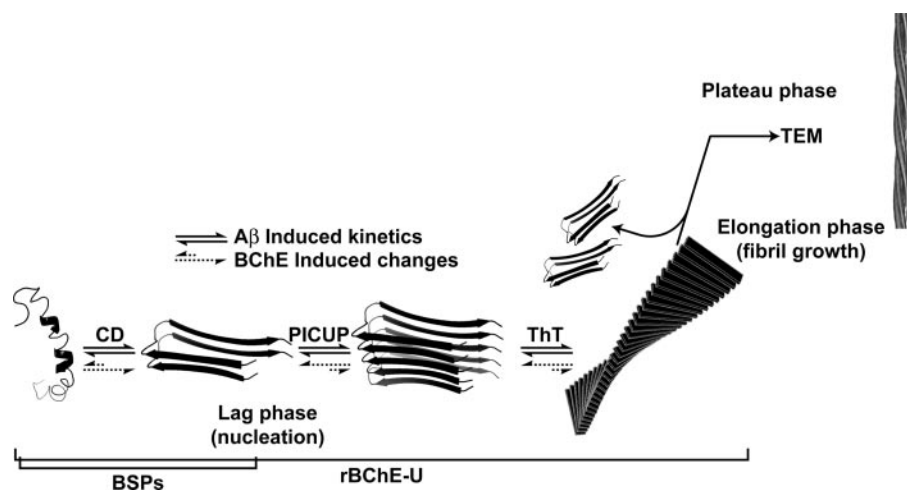
FIGURE 8. **BChE-induced changes in the Aβ accumulation process.** The Aβ aggregation pathway involves a set of mutually dependent reactions in complex equilibria (monomer ⇆ dimer ⇆ oligomer ⇆ fibril). The transition from helical structure to β-sheet conformation was studied by CD, oligomerization was followed by cross-linking, and fibril formation was tracked by ThT fluorescence and TEM. These reactions along the Aβ aggregation pathway are differentially affected by rBChE-U, BSP-U, and BSP-K.

ing AD onset. However, BChE-K was considerably less effective in attenuating the accumulation of Aβ fibrils than BChE-U. Although bearing in mind the alternative hypotheses for the role played by Aβ in AD, our findings suggest that BChE-K may pose either a risk or a protective factor in AD, in a context-dependent manner affected by other variables. It is conceivable that distinct population studies reflect these variables so that the null differences observed in the meta-analysis are less meaningful than the different population studies. Our findings attribute the association between BChE-K and AD progression to a structural origin, with dual activity: impaired stability and quaternary organization of BChE-K as compared with BChE-U and the consequently suppressed hydrolytic activity, counter-balanced by aberrant interactions with Aβ. This statement is supported by several considerations, as listed below.

The genetic implications of BChE-K in AD progression were studied comprehensively (supplemental Table ST2), but the location of the A539T polymorphism within the tetramerization domain of BChE (16, 17) has not been considered. Our current findings suggest that the BChE-K C-terminal substitution impairs both its stability and its intersubunit interactions. This is supported by findings where tetrameric serum BChE is thermostable, demonstrating that monomeric BChE loses hydrolytic activity within 10 min when incubated at 48 °C (49).

NMR detected chemical shift differences between BSP peptides upon adding PolyP. Nine residues in three regions of BSP-U showed chemical shift deviations ($\Delta\delta \geq 0.02$), as compared with only two BSP-K residues. Also, the changes observed in the BSP-U spectra upon binding PolyP were larger than those in the BSP-K spectra, indicating that PolyP induces greater organization in BSP-U. Changes in NMR chemical shift largely indicate those residues that undergo structural changes upon binding (*e.g.* Ref. 50). The distribution of BSP regions whose adjacent chemical environment changed, including the middle region and both termini, may indicate a change in the relative tilt of the helices or a motion in the hinge of the helix (at Gly-546/Gly-13) due to rearrangement of the kink. Such

motion may result from local helix disruption due to the A539T mutation; according to the Chou-Fasman parameters (51), alanine is one of the strongest helix stabilizers (helix propensity: 1.42), whereas threonine is one of the strongest β-sheet formers (β-sheet propensity: 1.19). One possible explanation of our findings is that threonine may slightly disrupt the helix or the amphiphilic distribution. The preference of threonine to form β-sheets is crucial in the context of amyloidogenic processes as all amyloid fibrils share a common cross-β-sheet structure. Another example of a disrupted helix originating from an alanine-to-threonine substitution is the solid-state NMR study that showed that the familial Parkinson disease-associated mutation A53T, which occurs in the N terminus of the amphiphilic helical α-synuclein, is more prone to forming β-structures than wild-type α-synuclein (52).

In BChE-K, the disrupted helix would likely be further desta-bilized by hydrogen bonding between Thr-539 and Glu-543, three amino acids away. Local unwinding of the helix could lead to loss of the ability of the adjacent pivotal tryptophan (Trp-541), which we previously demonstrated disrupts this amphiphilic helix, to attenuate Aβ fibril formation (25). Trp-541 contributes to structural interactions only when it is located at the polar face of an amphiphilic helix; if the helix becomes twisted or distorted, Trp-541 is no longer at the polar face, and the entire helix may cease to be amphiphilic.

Various Aβ aggregation pathways may exist simultaneously, and distinct inhibitors may affect only some of these. For instance, if oligomers are essential intermediates on the path-way to fibril formation, inhibitors that block oligomer forma-tion would ultimately block fibril formation as well. Alterna-tively, if fibrils and oligomers represent distinct aggregation pathways, some inhibitors might block oligomerization but not fibril formation and *vice versa*. We followed Aβ oligomeriza-tion by cross-linking, and we followed fibril formation by TEM. In both approaches, rBChE-U and BSP peptides attenuated both oligomer and fibril formation, albeit with different effi-ciencies. This tentatively implies that under the experimental conditions employed, oligomers are fibril intermediates. One possible explanation of the observed attenuation effects is that both rBChE-U and the BSP peptides can induce a shift of Aβ accumulation toward a stabilized Aβ oligomer, as large as 100-mer, if judged by the 1:100 molar ratio of effective inhibition (Fig. 8).

The amyloid hypothesis postulates that increased Aβ pro-duction and deposition plays a key role in triggering neuronal dysfunction and death in AD (15, 53). Many argue that the toxicity of Aβ lies in its soluble oligomeric intermediates (47, 48) rather than the insoluble fibrils that accumulate in AD plaques. Recent data indicate that small soluble oligomeric

forms, as short as dimers, are the main neurotoxic species involved in the pathogenesis of AD (17, 18). Our current findings indicate that neuroprotection may be achieved by shifting the equilibria of Aβ accumulation away from the potentially more hazardous oligomeric species, such as by BChE. In cross-linking and electron microscopy experiments, BSP peptides affected Aβ assembly less efficiently than rBChE-U. Also, BSP-K displayed less effective attenuation than BSP-U, possibly because it interacted with the Aβ monomers and/or intermediates less tightly. The differences in interactions are likely to be involved in the rBChE-U protection from Aβ neurotoxicity in cultured cells, where the peptides failed to provide protection.

The specific association between Aβ and the cell membrane has been shown to be the initial step in the chain of events that leads to toxicity (54). Our findings demonstrate that rBChE-U interacts with the neurotoxic Aβ oligomers, whereas Aβ-BSP interactions are much less effective. This is compatible with the hypothesis that BChE-U blocks the association of Aβ oligomers with the cell membrane. Therefore, BSP peptides are essential but are unable to promote such protection on their own. Furthermore, we demonstrated that the rBChE-U disruption extended to active fibril disassembly, compatible with a mechanism suggested by others (55), whereby inhibitor binding to the edge of the fibril leads to disassembly of the fibril by gradual strand removal. However, this mechanism requires high ratios of inhibitor to Aβ and therefore does not fit the 1:100 ratio we observed, in which a single rBChE-U molecule can initiate breakdown of large Aβ oligomers. Rather, our results suggest that the symmetry between the layers is broken by steric hindrance, which induces structural instabilities due to the Ala to Thr mutation and leads to collapse of the entire structure of the fibril. The same structural features that destabilize BChE-K are therefore those that make it less effective as a neuroprotector.

REFERENCES

1. Gómez-Ramos, P., and Morán, M. A. (1997) *Mol. Chem. Neuropathol.* **30,** 161–173
2. Carson, K. A., Geula, C., and Mesulam, M. M. (1991) *Brain Res.* **540,** 204–208
3. Guillozet, A. L., Smiley, J. F., Mash, D. C., and Mesulam, M. M. (1997) *Ann. Neurol.* **42,** 909–918
4. Perry, E. K., Perry, R. H., Blessed, G., and Tomlinson, B. E. (1978) *Neuropathol. Appl. Neurobiol.* **4,** 273–277
5. Morán, M. A., Mufson, E. J., and Gómez-Ramos, P. (1993) *Acta Neuropathol.* **85,** 362–369
6. Wright, C. I., Geula, C., and Mesulam, M. M. (1993) *Ann. Neurol.* **34,** 373–384
7. Lansbury, P. T., Jr. (1992) *Biochemistry* **31,** 6865–6870
8. Lomakin, A., Chung, D. S., Benedek, G. B., Kirschner, D. A., and Teplow, D. B. (1996) *Proc. Natl. Acad. Sci. U. S. A.* **93,** 1125–1129
9. Shen, J., and Kelleher, R. J., 3rd (2007) *Proc. Natl. Acad. Sci. U. S. A.* **104,** 403–409
10. Praticò, D. (2008) *Ann. N.Y. Acad. Sci.* **1147,** 70–78
11. Bush, A. I., and Tanzi, R. E. (2008) *Neurotherapeutics* **5,** 421–432
12. Zhu, X., Raina, A. K., Perry, G., and Smith, M. A. (2004) *Lancet Neurol.* **3,** 219–226
13. Mancuso, M., Coppèdè, F., Murri, L., and Siciliano, G. (2007) *Antioxid. Redox Signal.* **9,** 1631–1646
14. Lee, H. G., Casadesus, G., Zhu, X., Takeda, A., Perry, G., and Smith, M. A. (2004) *Ann. N.Y. Acad. Sci.* **1019,** 1–4
15. Hardy, J., and Selkoe, D. J. (2002) *Science* **297,** 353–356
16. Altamirano, C. V., and Lockridge, O. (1999) *Chem. Biol. Interact.* **119–120,** 53–60
17. Blong, R. M., Bedows, E., and Lockridge, O. (1997) *Biochem. J.* **327,** 747–757
18. Perrier, A. L., Massoulié, J., and Krejci, E. (2002) *Neuron* **33,** 275–285
19. Bon, S., Ayon, A., Leroy, J., and Massoulié, J. (2003) *Neurochem. Res.* **28,** 523–535
20. Li, H., Schopfer, L. M., Masson, P., and Lockridge, O. (2008) *Biochem. J.* **411,** 425–432
21. Nicolet, Y., Lockridge, O., Masson, P., Fontecilla-Camps, J. C., and Nachon, F. (2003) *J. Biol. Chem.* **278,** 41141–41147
22. Ngamelue, M. N., Homma, K., Lockridge, O., and Asojo, O. A. (2007) *Acta Crystallogr. F Struct. Biol. Cryst. Commun.* **63,** 723–727
23. Dvir, H., Harel, M., Bon, S., Liu, W. Q., Vidal, M., Garbay, C., Sussman, J. L., Massoulié, J., and Silman, I. (2004) *EMBO J.* **23,** 4394–4405
24. Bartels, C. F., Jensen, F. S., Lockridge, O., van der Spek, A. F., Rubinstein, H. M., Lubrano, T., and La Du, B. N. (1992) *Am. J. Hum. Genet.* **50,** 1086–1103
25. Diamant, S., Podoly, E., Friedler, A., Ligumsky, H., Livnah, O., and Soreq, H. (2006) *Proc. Natl. Acad. Sci. U. S. A.* **103,** 8628–8633
26. Baden, E. M., Owen, B. A., Peterson, F. C., Volkman, B. F., Ramirez-Alvarado, M., and Thompson, J. R. (2008) *J. Biol. Chem.* **283,** 15853–15860
27. Hurshman Babbes, A. R., Powers, E. T., and Kelly, J. W. (2008) *Biochemistry* **47,** 6969–6984
28. O'Brien, K. K., Saxby, B. K., Ballard, C. G., Grace, J., Harrington, F., Ford, G. A., O'Brien, J. T., Swan, A. G., Fairbairn, A. F., Wesnes, K., del Ser, T., Edwardson, J. A., Morris, C. M., and McKeith, I. G. (2003) *Pharmacogenetics* **13,** 231–239
29. Lopez, O. L., Becker, J. T., Wisniewski, S., Saxton, J., Kaufer, D. I., and DeKosky, S. T. (2002) *J. Neurol. Neurosurg. Psychiatry* **72,** 310–314
30. Ghebremedhin, E., Thal, D. R., Schultz, C., and Braak, H. (2002) *Neurosci. Lett.* **320,** 25–28
31. Holmes, C., Ballard, C., Lehmann, D., David Smith, A., Beaumont, H., Day, I. N., Nadeem Khan, M., Lovestone, S., McCulley, M., Morris, C. M., Munoz, D. G., O'Brien, K., Russ, C., Del Ser, T., and Warden, D. (2005) *J. Neurol. Neurosurg. Psychiatry* **76,** 640–643
32. Bertram, L., McQueen, M. B., Mullin, K., Blacker, D., and Tanzi, R. E. (2007) *Nat. Genet.* **39,** 17–23
33. Arendt, T., Brückner, M. K., Lange, M., and Bigl, V. (1992) *Neurochem. Int.* **21,** 381–396
34. Ben Assayag, E., Bova, I., Berliner, S., Peretz, H., Usher, S., Shapira, I., and Bornstein, N. M. (2006) *Thromb. Haemost.* **95,** 428–433
35. Gätke, M. R., Viby-Mogensen, J., and Bundgaard, J. R. (2002) *Scand. J. Clin. Lab. Invest.* **62,** 375–383
36. Ofek, K., Krabbe, K. S., Evron, T., Debecco, M., Nielsen, A. R., Brunnsgaad, H., Yirmiya, R., Soreq, H., and Pedersen, B. K. (2007) *J. Mol. Med.* **85,** 1239–1251
37. Karnovsky, M. J., and Roots, L. (1964) *J. Histochem. Cytochem.* **12,** 219–221
38. Berson, A., Knobloch, M., Hanan, M., Diamant, S., Sharoni, M., Schuppli, D., Geyer, B. C., Ravid, R., Mor, T. S., Nitsch, R. M., and Soreq, H. (2008) *Brain* **131,** 109–119
39. Piotto, M., Saudek, V., and Sklenár, V. (1992) *J. Biomol. NMR* **2,** 661–665
40. Wagner, R., and Berger, S. (1996) *J. Magn. Reson. A* **123,** 119–121
41. Wüthrich, K. (1986) *NMR of Proteins and Nucleic Acids*, John Wiley & Sons, New York
42. Fancy, D. A., and Kodadek, T. (1999) *Proc. Natl. Acad. Sci. U. S. A.* **96,** 6020–6024
43. Podoly, E., Bruck, T., Diamant, S., Melamed-Book, N., Weiss, A., Huang, Y., Livnah, O., Langermann, S., Wilgus, H., and Soreq, H. (2008) *Neurodegener. Dis.* **5,** 232–236
44. Whitmore, L., and Wallace, B. A. (2004) *Nucleic Acids Res.* **32,** W668–673
45. Bergmeyer, H. U., Bernt, E., and Hess, B. (1963) in *Methods of Enzymatic*

Analysis (Bergmeyer, H. U., ed), pp. 736–743, Academic Press, New York, NY

46. Huang, Y. J., Huang, Y., Baldassarre, H., Wang, B., Lazaris, A., Leduc, M., Bilodeau, A. S., Bellemare, A., Côté, M., Herskovits, P., Touati, M., Turcotte, C., Valeanu, L., Lemée, N., Wilgus, H., Bégin, I., Bhatia, B., Rao, K., Neveu, N., Brochu, E., Pierson, J., Hockley, D. K., Cerasoli, D. M., Lenz, D. E., Karatzas, C. N., and Langermann, S. (2007) *Proc. Natl. Acad. Sci. U. S. A.* **104,** 13603–13608

47. Dahlgren, K. N., Manelli, A. M., Stine, W. B., Jr., Baker, L. K., Krafft, G. A., and LaDu, M. J. (2002) *J. Biol. Chem.* **277,** 32046–32053

48. Klein, W. L., Stine, W. B., Jr., and Teplow, D. B. (2004) *Neurobiol. Aging* **25,** 569–580

49. Edwards, J. A., and Brimijoin, S. (1983) *Biochim. Biophys. Acta* **742,** 509–516

50. Tidow, H., Melero, R., Mylonas, E., Freund, S. M., Grossmann, J. G., Carazo, J. M., Svergun, D. I., Valle, M., and Fersht, A. R. (2007) *Proc. Natl. Acad. Sci. U. S. A.* **104,** 12324–12329

51. Chou, P. Y., and Fasman, G. D. (1974) *Biochemistry* **13,** 211–222

52. Heise, H., Celej, M. S., Becker, S., Riedel, D., Pelah, A., Kumar, A., Jovin, T. M., and Baldus, M. (2008) *J. Mol. Biol.* **380,** 444–450

53. Glabe, C. (2001) *J. Mol. Neurosci.* **17,** 137–145

54. Demuro, A., Mina, E., Kayed, R., Milton, S. C., Parker, I., and Glabe, C. G. (2005) *J. Biol. Chem.* **280,** 17294–17300

55. Soto, P., Griffin, M. A., and Shea, J. E. (2007) *Biophys. J.* **93,** 3015–3025

56. Arpagaus, M., Kott, M., Vatsis, K. P., Bartels, C. F., La Du, B. N., and Lockridge, O. (1990) *Biochemistry* **29,** 124–131